

Studies on crystallization and domain structure of a ferromagnetic amorphous alloy $\text{Co}_{90}\text{Zr}_{10}$

A. J. JANICKI, H. MATYJA

Institute of Materials Science and Engineering, Warsaw Technical University, 02-524 Warsaw, Narbutta 85, Poland

The paper presents the first results of studies on crystallization and domain structure of a new ferromagnetic amorphous alloy $\text{Co}_{90}\text{Zr}_{10}$. Amorphous Co-Zr alloys were obtained by the "piston and anvil" method with 20 to 45 at % of Co and 90 at % of Zr. Crystallization of $\text{Co}_{90}\text{Zr}_{10}$ was studied by X-ray diffraction and differential calorimetry, as well as by transmission electron microscopy (TEM) with simultaneous heating of the material. Domain structure in the amorphous phase was investigated by the method of Lorentz. The types of structures occurring were described, domain wall widths were calculated, and the direction of changes in the parameters of the magnetic structure — caused by annealing and phase transformation — was suggested.

1. Method

A series of Co-Zr alloys was prepared by arc melting in argon atmosphere gettered by melted titanium. The alloys were several times remelted for homogeneity, whereupon the percentage composition was verified chemically; the deviation from the intended composition did not exceed 0.7 at %.

Rapid cooling of the alloys from the liquid state was performed by the piston and anvil technique. The amorphous structure of samples was verified by X-ray diffraction, as well as directly using an electron microscope, because some regions of the samples were sufficiently thin.

Crystallization processes were investigated during continuous heating in a DSC-2 Perkin-Elmer microcalorimeter at a rate of 5 to 80 K min^{-1} . An activation energy for the crystallization process was determined according to Kissinger [1]. A Philips EM 300 transmission electron microscope enabled the crystallizing phases to be identified, using Lorentz and Fresnel's method of contrast to show magnetic domain structures, and to allow the domain wall widths to be calculated.

2. Result and discussion

The glass formation range obtained in TM-TM

type binary alloys $\text{Co}_x\text{Zr}_{100-x}$ amounted to $x = 20$ to 45 at % and 90 at %.

At room temperature and higher temperatures, only the amorphous alloy $\text{Co}_{90}\text{Zr}_{10}$ exhibited ferromagnetic properties.

2.1. Crystallization of $\text{Co}_{90}\text{Zr}_{10}$

Values of the temperatures of onset of crystallization, T_x , crystallization peak T and glass-formation T_g at various heating rates are shown in Table I.

Fig. 1 presents the calorimetric course of heating at a rate of 5 K min^{-1} , and also indicates the corresponding phases.

During heating at a rate of 5 K min^{-1} , crystallization of fcc β -Co begins at 772 K, followed by that of stable $\text{Co}_{23}\text{Zr}_6$ at 792 K. The activation

TABLE I Values of temperatures T_x , T , T_g for $\text{Co}_{90}\text{Zr}_{10}$ foil heated at various rates

Heating rate (K min^{-1})	T_g (K)	T_{x1} (K)	T_1 (K)	T_{x2} (K)	T_2 (K)
5	—	772	783	792	796
20	—	—	—	808	815
40	—	—	—	820	837
80	802	—	—	825	845

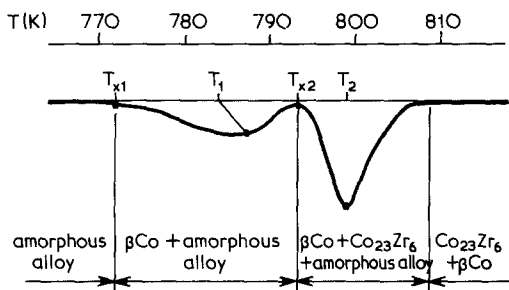


Figure 1. DSC curve of amorphous alloy $\text{Co}_{90}\text{Zr}_{10}$, heating rate 5 K min^{-1} , and corresponding phases.

energy for this process, calculated according to Kissinger's method was $2.55 \pm 0.1 \text{ eV}$.

In the course of cooling to about 650 K, some of the β -Co is transformed into hcp α -Co, so that at room temperature the phases α -Co, β -Co, $\text{Co}_{23}\text{Zr}_6$ occur together.

Crystallization of $\text{Co}_{90}\text{Zr}_{10}$ was also investigated by transmission electron microscopy (TEM), using a holder for sample heating in the microscope. Below 700 K the specimen remains amorphous (Fig. 2).

At 710 K the strongest [111] reflection of fcc β -Co appears, indicating that formation of β -Co by crystallization has begun. The first crystals of phase $\text{Co}_{23}\text{Zr}_6$ appear at about 745 K with fcc structure and $a_0 = 11.516 \text{ \AA}$ [2] (Fig. 3).

The mixture of crystals of fcc Co and $\text{Co}_{23}\text{Zr}_6$ in the amorphous matrix is shown in Fig. 4. Progressive growth of crystals is observed. Further heating at about 5 K min^{-1} to 800 K causes complete crystallization of the alloy (Fig. 5). After cooling to about 300 K crystals of $\text{Co}_{23}\text{Zr}_6$, with both fcc and hcp Co, are present. The initial occurrence of separated crystals and their later

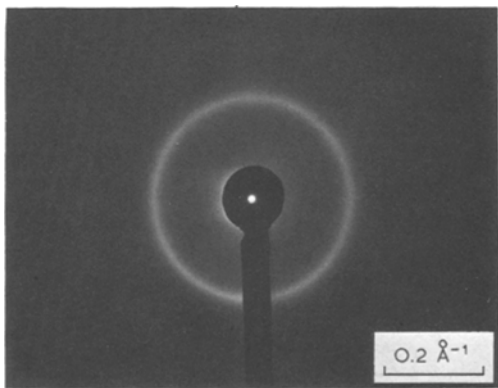


Figure 2. Electron microscopic diffraction of $\text{Co}_{90}\text{Zr}_{10}$ foil at 680 K.

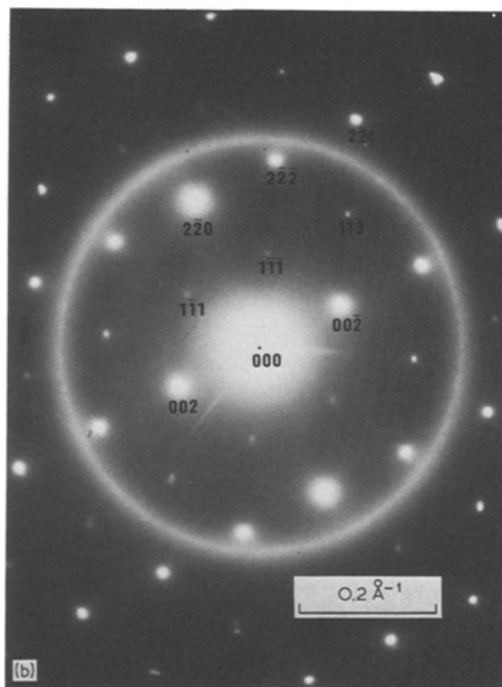
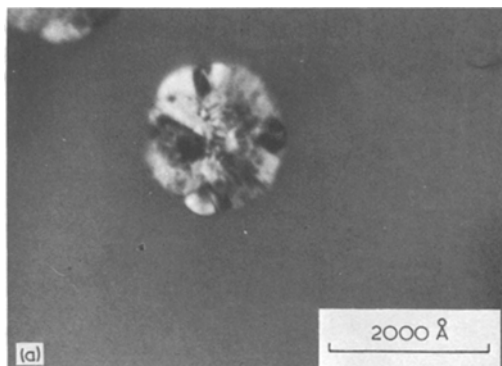


Figure 3. (a) Crystal of $\text{Co}_{23}\text{Zr}_6$ in amorphous environment, $T = 750 \text{ K}$ and (b) diffraction, fcc, structure, crystal orientation [110], $a_0 = 11.516 \text{ \AA}$.

$F_{hkl} = 4f_{\text{Co}} - f_{\text{Zr}}$ for $h + k + l = 2n + 1$ and $4f_{\text{Co}} + f_{\text{Zr}}$ for $h + k + l = 2n$ therefore the reflexes with odd hkl are less intense.

growth suggests that crystallization proceeds by nucleation and growth. Differences in crystallization temperatures between both DSC and TEM methods result from dissimilar conditions of heating of the material.

2.2. Domain structure in $\text{Co}_{90}\text{Zr}_{10}$

Observations of the domains were carried out by the TEM method and Fresnel's contrast. The amorphous materials exhibit strip, cross-tie and ripple structures. The cross-tie structure (Figs. 6a

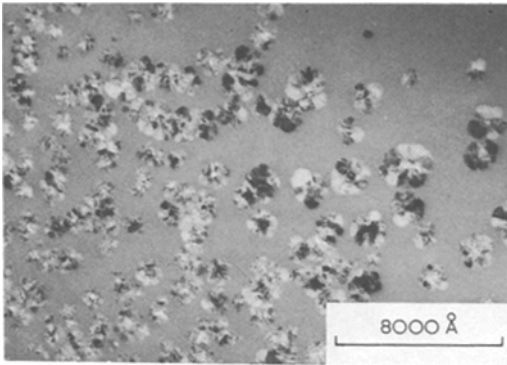


Figure 4. Crystals of $\text{Co}_{23}\text{Zr}_6$ and Co fcc in foil annealed for 10 min at $T = 650\text{ K}$.

and b), characterized by lines with transverse bands, often appears in thin foils. This picture testifies to the occurrence of a combination of walls of Néel and Bloch [3] types, in which a change in the direction of the magnetic moment vector takes place in the plane of the layer (Néel's wall) and in the plane perpendicular to the layer (Bloch's wall) (Fig. 7). The ripple structure is visible in Figs. 6a, b and 8a, b. Characteristic lines

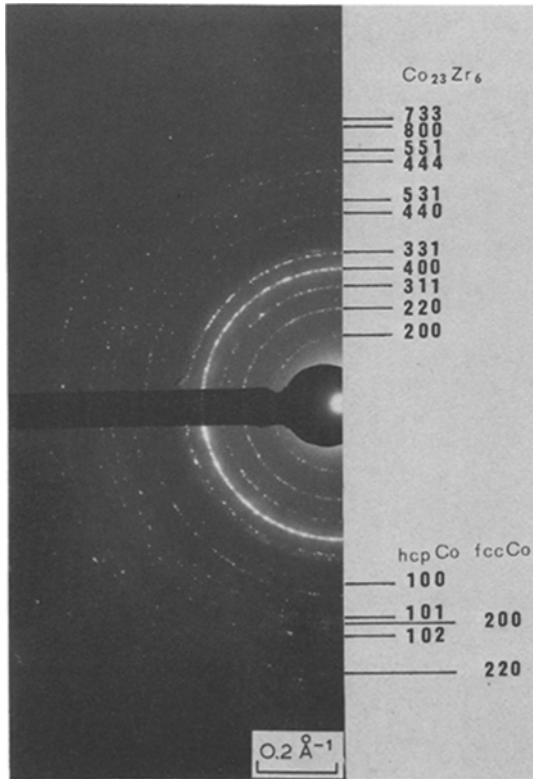


Figure 5. Diffraction of alloy $\text{Co}_{90}\text{Zr}_{10}$ being completely crystalline after cooling to room temperature.

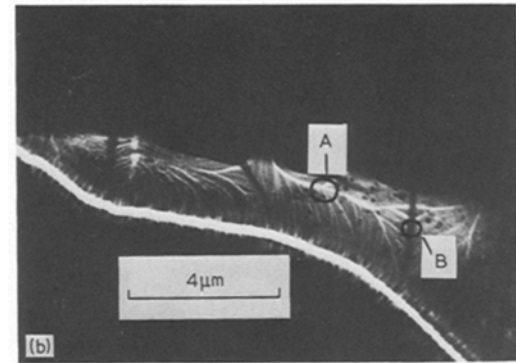
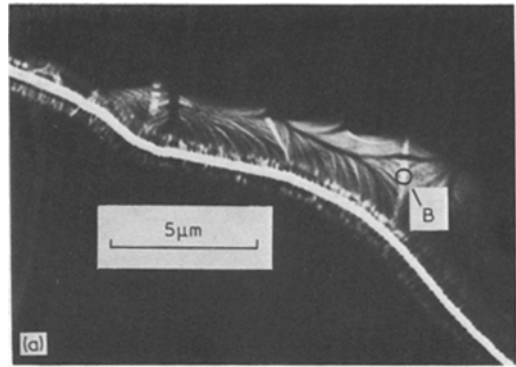


Figure 6. Domain structures in amorphous foil $\text{Co}_{90}\text{Zr}_{10}$ (a) $\delta_w = 250\text{ Å}$; $z = -5.3\text{ mm}$, (b) 6 mm.

with reduced magnetic field intensity can be seen within the domains.

Divergent wall width (dark) w_d and convergent wall width (light) w_c were measured with a microdensitometer, and the real domain wall width $\delta_w = (w_d - w_c)/2$ was calculated. This domain wall width determination is subject to error owing to several factors:

(a) lines within the domains cause fluctuation of δ_w ; there is no distinct contrast boundary, particularly for the ripple structure (Figs. 6b and 8b, detail A).

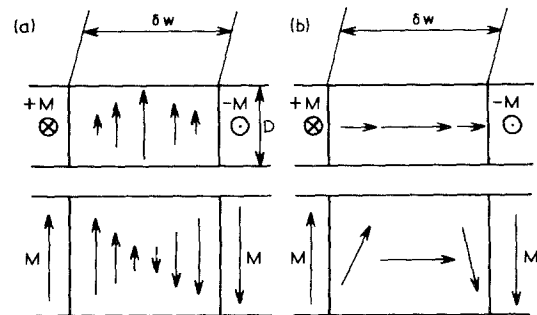


Figure 7. Vector of magnetic moment in (a) Bloch's and (b) Néel's walls.

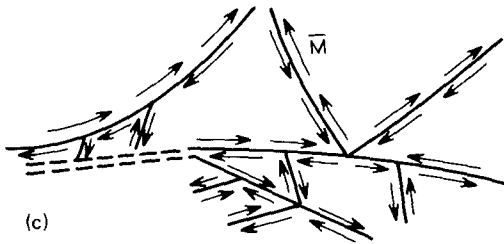
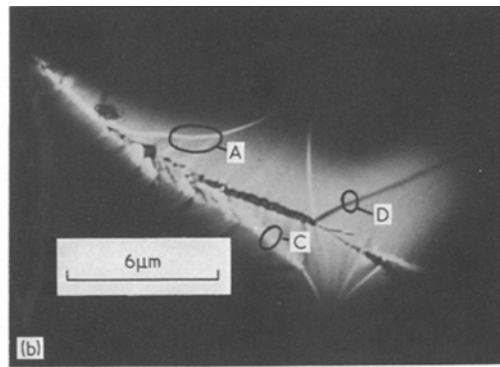
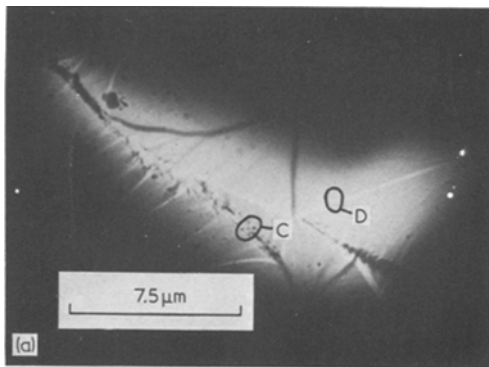


Figure 8. Domain structures in amorphous foil $\text{Co}_{90}\text{Zr}_{10}$, (a) $\delta_w = 310 \text{ \AA}$; $z = -6.5 \text{ mm}$, (b) 7.1 mm . (c) Proposed distribution of magnetizing vector \vec{M} within the domain region.

(b) lines perpendicular to the mean direction of magnetization run towards the walls under different angles. This causes local fluctuations of the wall width which is entirely dependent on the complete change in the angle of spin across the wall [4].

Moreover, Figs. 6a and b show a fragment of the strip structure, at site *B*, $\delta_w = 250 \text{ \AA}$; while detail *C* in Figs. 8a and b shows the complex structure of walls, due to interference effects. At site *D*, measured δ_w amounts to 310 \AA . Fig. 8c shows the proposed distribution of magnetizing vector \vec{M} in the material. The values of magnifications M and of the out-of-focus distances z , necessary for interpretation of the pictures, are given.

Initial studies of the domain structure, mainly of the domain wall width and thus of the energy of the domain walls, together with simultaneous annealing of the material, testify to a dependence of wall energy on the crystalline state of the materials [5, 6].

Annealing of amorphous ferromagnetic material,

as well as processes of crystallization and phase transformations cause changes in wall energy and domain size.

Acknowledgements

The authors are greatly indebted to Professor T. Egami and Dr. H. Jones for valuable discussion of the results, as well as to J. Ostatek, M. S., and M. Kijek, M.S., for help in the selection of alloys and in their preparation.

This work was supported by Ministry of Science, High Education and Technology (Grant No. M.R.-I.21).

References

1. H. E. KISSINGER, *Anal. Chem.* **29** (1959) 1702.
2. Powder Diffraction File, Inorganic 1973, Joint Committee on Powder Diffraction Standards, Swarthmore, PA.
3. A. HUBERT in "Theorie der Domänenwände in geordneten Medien" (Springer Verlag, Berlin, Heidelberg and New York, 1974).
4. R. H. WADE, *Proc. Phys. Soc.* **79** (1962) 1237.
5. A. J. JANICKI, Thesis, Warsaw Technical University, Poland (1980).
6. H. MATYJA, Conference on Metallic Glasses, Budapest, Hungary (1980).

Received 17 January and accepted 6 February 1980.